

FEDSM-ICNMM2010-30524

NETWORK ANALYSIS OF NON-UNIFORMLY HEATED EVAPORATIVE MICRO-CHANNEL SYSTEMS

Hee Joon Lee

Center for Automation Technologies and Systems
Rensselaer Polytechnic Institute
Troy, NY 12180, USA

Shi-chune Yao

Dept. of Mechanical Engineering
Carnegie Mellon University
Pittsburgh, PA 15213, USA

ABSTRACT

A network analysis was established to model the array of evaporative micro-channels with possible non-uniformity heating as well as branching of the channels. Iterative solution of the evaporative micro-channel network can be obtained using the Hardy-Cross method together with accurate two-phase head-loss correlations. Based on the experimental evidence, cross-cutting micro-channels reduce the uneven flow distribution in parallel micro-channels at non-uniform heating. Through this network analysis, it is also evident that cross-cutting grooves on parallel micro-channels are effective in reducing non-uniform heating effects and enhancing the uniform wall temperature distribution.

INTRODUCTION

Arrays of two-phase micro-channels have been applied in the cooling system of high power electronics, flow passages in fuel cells, and heat exchangers in energy and petroleum industries. Although evaporative parallel micro-channels have a great advantage of high heat transfer coefficient, when non-uniform heating occurs it frequently shows uneven distribution of the coolant among the channels and severe flow instabilities. It is desirable to explore alternative designs which could avoid flow instabilities and minimize the uneven flow distribution in parallel evaporative micro-channels at non-uniform heating.

Lee et al. [1] investigated alternative designs of evaporative micro-channel systems, such as expanding channels or inlet orifices, which are inherently stable of two-phase flow oscillation over wide range of operational conditions. Another potential approach is to relieve the explosive expansion bubbles at hot spots in micro-channels by providing cross-cutting grooves on parallel micro-channels. Through cross-cutting grooves the explosive flows in a micro-channel communicate with other adjacent channels. The width of the groove was made to be greater than the width of the

micro-channels that the vapor bubbles in the micro-channels will tend to migrate into the cross-cutting grooves due to the differential surface tension force. Then, the two-phase fluids run into the downstream section of the micro-channels rather uniformly.

Most micro-channel systems may have a non-uniform heating boundary condition from its local heat sources. For example, the microprocessor of modern-electronics incorporates all of the functions of a central processing unit (CPU) on a single integrated circuit (IC). The IC consists of many zones of electronic functions such as logic, memory, and power-conditioning etc. According to the region of the functionalities in IC, a microprocessor generates non-uniform heat to its surroundings. For the cooling of such a non-uniformly heated evaporative micro-channel system, the detail design of an appropriate system becomes extremely difficult. A general and powerful design tool to support the evaluations of design alternatives and detail configurations is strongly needed. To support the quantitative design of evaporative micro-channel systems with complex channel configurations and non-uniform heating, computational scheme for a network system was developed in this paper. Network models of single phase flow in pipe systems have been well established in mechanical and chemical engineering applications [2]. The basic idea of channel network models is that the head-loss around any loop of piping must be zero. Recently, Lee and Yao [3] expanded this channel network models to evaporative micro-channel systems. They calculated two-phase head losses and applied these to two-phase evaporative micro-channel network calculation. Comparing straight and expanding mini-channels, expanding mini-channels shows more uniform flow rate distribution due to lower head loss than straight mini-channels. Cho et al. [4] investigated flow rate and wall temperature on 33 parallel micro-channels (300 μm hydraulic diameter) with

NOMENCLATURE

A	Area [m ²]
Bo	Bond number
C	Chisholm parameter
D	Channel hydraulic diameter [m]
f	Friction factor
G	Mass flux [kg/m ² /s]
g	The acceleration of gravity [m/s ²]
h	Heat transfer coefficient [W/m ² /K]
h_L	Head loss [m]
i	Latent heat [J/kg]
K	Loss coefficient [s ² /m ⁵]
k	Thermal conductivity [W/m/K]
L	Channel length [m]
P	Perimeter [m]
p	Pressure [Pa]
Q	Flow rate [m ³ /s]
\dot{q}	Heat rate [W]
R	Instability parameter
T	Temperature [°C]
X	Martinelli number
x	Thermodynamic quality
z	Local position along the channel [mm]

Greek symbols

α	Void fraction
Δ	Difference
ε	Fin effectiveness
ϕ	Two-phase frictional multiplier
ρ	Density [kg/m ³]
ν	Specific volume [m ³ /kg]

Subscripts

acc	Accelerational
b	Base
ch	Bottom surface of micro-channel
f	Liquid
fin	Fin
$fric$	Frictional
g	Vapor
i	Index
in	Inlet of test section
out	Outlet of test section
SAT	Saturation
sp	Single phase
$total$	Total
tp	Two-Phase

different inlet and outlet header providing either uniform or non-uniform heat flux experimentally. They reported that the diverging micro-channels with trapezoidal header showed the smallest pressure drop, but the non-uniformity of wall temperature increased.

In this paper, instead of single phase head-losses, two-phase head-losses of micro-channels were used [3]. Then, the Hardy-Cross method was applied to iteratively searching for the solution of an evaporative micro-channel network. Furthermore, the stability criteria of evaporative micro-channels are also applied in the design analysis. The network algorithm applied to both the parallel and the cross-cutting micro-channels was presented and implemented. Experimental evidence and the prediction of network analysis of the advantage of cross-cutting grooves in evaporative micro-channel systems was demonstrated for non-uniformity heated evaporative micro-channel systems.

EVAPORATIVE MICRO-CHANNEL NETWORK

Modeling

Evaporative micro-channel network was only applied to a heat sink which has channel pattern on a testbed and evaporation inside channels. Therefore, a pump and other hydraulic components of the system was neglected to be considered. The main principle of channel network models is that the head loss, h_L around any single pipe loop in micro-channels must be zero in Eq. (1).

$$\sum_i h_L = \sum_i K_i Q_i^2 = 0 \quad (1)$$

In addition, the solution to a network should satisfy continuity and energy conservations. Applying these formulations to each loop and pipe junction should give a series of simultaneous equations to be solved together.

This existing flow network analysis method of single-phase flows was extended to cover the two-phase evaporative flow network. To design the evaporative micro-channel network systems, network calculation shall be performed for two-phase pressure losses in micro-channels. If the micro-channel is horizontally positioned, the gravitational pressure drop can be negligible.

The total two-phase head-loss in a horizontal micro-channel can be obtained in terms of the pressure drops of single phase and two-phase zone. Two-phase pressure drop had frictional pressure drop, due to shear stresses at the wall and the interface between phases, and acceleration pressure drop, due to the local average density change as the local quality increases.

$$h_L = (K_{sp} + K_{tp,fric} + K_{tp,acc})Q^2 \quad (2)$$

where

$$K_{sp} = f \frac{L}{2gDA^2} \quad (3)$$

$$K_{tp,fric} = \frac{1}{(x_{out} - x_{in})} \int_{x_{in}}^{x_{out}} \frac{f_f P(1-x)^2}{2A^3 g} \phi^2 dx \quad (4)$$

$$K_{tp,acc} = \frac{1}{A^2 v_f g} \left[\begin{array}{c} \left[\frac{x_{out}^2 v_g}{\alpha_{out}} + \frac{(1-x_{out})^2 v_f}{(1-\alpha_{out})} \right] \\ - \left[\frac{x_{in}^2 v_g}{\alpha_{in}} + \frac{(1-x_{in})^2 v_f}{(1-\alpha_{in})} \right] \end{array} \right] \quad (5)$$

The accurate and generalized two-phase correlation of frictional pressure drop in a micro-channel for general design purposes was applied in the two-phase multiplier, ϕ in Eq. (4) [5]. Two-phase frictional pressure drop does not only add up each single phase of liquid and vapor, but also the interfacial interaction between phases denoted by the Chisholm parameter, C . The two-phase multiplier is a function of the Chisholm parameter and the Martinelli number, X , the ratio of pressure drop of each phase shown in Eqs. (6) and (7).

$$\phi^2 = 1 + \frac{C}{X} + \frac{1}{X^2} \quad (6)$$

$$X^2 = \left(\frac{dp}{dz} \Big|_{fric} \right)_f / \left(\frac{dp}{dz} \Big|_{fric} \right)_g \quad (7)$$

Lee et al. [5] reported that the Bond number and the outlet quality should be considered as important variables in a micro-channel to correlate the Chisholm parameter,

$$C = 121.6 [1 - \exp(-22.7Bo)] x_{out}^{1.85} \quad (8)$$

To iterate the solution of an evaporative micro-channel network, the Hardy-Cross method was adopted [2]. The Hardy-Cross method perturbs a very small flow rate (ΔQ) in each micro-channel. This perturbation is updated by iterations until the solution converges simultaneously.

$$\sum_{i=1}^N K_i (Q_i + \Delta Q)^2 = 0 \quad (9)$$

$$\Delta Q = \frac{\sum_{i=1}^N K_i Q_i^2}{-2 \sum_{i=1}^N K_i Q_i} \quad (10)$$

On the other hand, evaporative micro-channels may encounter flow instabilities that steady operations could become difficult. These instabilities are created by a growing bubble in the narrow channel which is severely confined that it expands toward both upstream and downstream simultaneously in an evaporative micro-channel. The static model of flow instability was included in the channel network algorithm. A generalized static model of instability has been proposed by Lee et al. [1] considering the force balances on a liquid-vapor interface of a growing bubble in terms of evaporation momentum change, inertia and surface tension in a micro-channel. For parallel micro-channels without channel expansion and inlet orifice, the ratio of the back flow force and the forward flow inertia can be expressed as the instability parameter, R , as

$$R = \frac{\dot{q}_{total}}{2Ai_{fg}G} \sqrt{\frac{\rho_f}{\rho_g}} \quad (11)$$

When the instability parameter R is greater than unity, it means the flow is fluctuating because the back flow force of a growing bubble is greater than the forward liquid inertia. Therefore, R should be less than unity at everywhere to achieve a stable evaporative micro-channel system when evaporate channel network was solved by Eqs. (1) – (10). Equation (11) is most important for system with very low Bond number (channel diameter is much lower than nominal bubble size) working fluids such as water, where a generated bubble is severely squeezed by the narrow channel toward both up and downstreams. For design of a stable evaporative micro-channel network system, the computational results of the channel network should be satisfied with the stable criterion of the channel flow instability model in Eq. (11).

The generalized two-phase correlation of heat transfer for general design purposes was adopted to calculate the two-phase heat transfer coefficient [5]. Lee et al.'s generalized heat transfer correlation [5] is based upon the Lee and Mudawar's heat transfer correlation [6] by multiplying a factor

$$h_{tp} = \frac{h_{tp, Lee-Mudawar}}{0.958 \exp(-Bo/1.537) + 0.126} \quad (12)$$

Moreover, total heat supplied from heater was dissipated by convective channel flow and the fin between micro-channels. The heat rates of the fin base (the wall between adjacent micro-channels acts like a fin) and the bottom surface of a micro-channel was obtained by fin effectiveness, ε_{fin} as [7]

$$\dot{q}_{ch} = \dot{q}_{total} - \dot{q}_{fin} = \dot{q}_{total} / (1 + \varepsilon_{fin}) = h_{tp} A_{ch} (T_{ch} - T_{SAT})$$

where $\varepsilon_{fin} = \sqrt{\frac{kP}{h_{tp} A_c}}$ (13)

The bottom wall temperature of micro-channels, T_{ch} could be calculated from Eq. (13). Then, assuming adiabatic tip boundary condition, the wall temperature at the fin base, T_b was obtained by

$$\dot{q}_{fin} = \varepsilon_{fin} h_{ip} A_b (T_b - T_{SAT}) \tanh\left(\sqrt{\frac{h_{ip} P}{k A_b}} L\right) \quad (14)$$

The material of the fin base and fin is Aluminum 2024 (thermal conductivity 190 W/m/K). Typically, using the condition of 7 W/cm² heat flux and 41.8 kg/m²/s mass flux of water in parallel micro-channels with uniform heating, the heat transfer coefficient, the fin efficiency, and the wall temperature of both micro-channels and fins are about 40,000 W/m²/K, 60~70 %, and 102.6°C, respectively.

Validation

Evaporative micro-channel network modeling was validated against the existing simulation result of Cho et al. [4]. They fabricated a silicon micro-channel heat sink with 33 rectangular shaped parallel micro-channels constructed with 300 μm hydraulic diameter and 20 mm length. The wall thickness between micro-channels was 200 μm. There was a rectangular header (5 mm wide). R123 was used as a working fluid. Saturated liquid ($x=0$) comes into the inlet header and distributes to 33 parallel micro-channels. The mass flow rate and the uniform heat flux were 0.18 g/s and 40 kW/m², respectively.

The normalized mass flow distribution in straight micro-channels with rectangular headers at uniformly heating [4] shown in Fig. 1 was selected to validate the current evaporative micro-channel network modeling. Since the authors did not provide system pressure and inlet conditions, the system pressure was assumed to be 111.5 kPa due to the use of two syringe pumps. The geometry was modeled by 32 loops and 97 channels (33 micro-channels and 64 segments of headers). Saturated liquid comes into the channel 1 and drains from the channel 33.

Figure 1 shows the comparison of normalized mass flow distribution in 33 micro-channels between the current simulation and the result from Cho et al. [4]. Since the exit of the outlet header is near the channel 33, the two-phase flow leaving the channel 1 has a longer distance to travel than the channel 33. Therefore, the two-phase head loss of the flow passing through the channel 1 is larger, and the mass flow rate becomes less. The trend predicted in the simulation is similar to the observation of Cho et al. [4] as shown in Fig. 1. The slight discrepancy may due to the assumptions made on the unknown system pressure and inlet conditions.

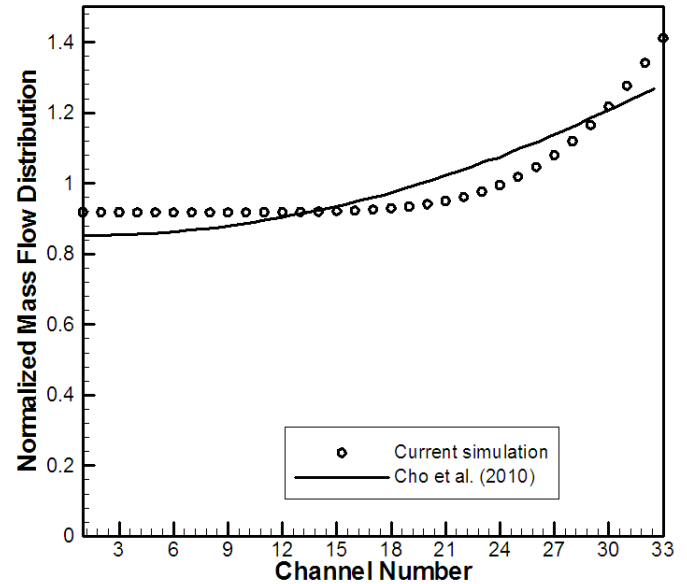


FIGURE 1. COMPARISON OF CURRENT EVAPORATIVE MICRO-CHANNEL NETWORK MODELING AND SIMULATION RESULT (Cho et al. [4]) IN STRAIGHT PARALLEL MICRO-CHANNELS WITH RECTANGULAR HEADER

EXPERIMENTAL OBSERVATION

Lee et al. [1] conducted flow instability experiments in micro-channel systems of boiling water. As shown in Fig. 2, a bidirectional syringe pump supplies 90°C distilled and degassed water. To prevent flow discontinuity when the syringe pump changes direction and to maintain a constant pressure, a pressure regulator in the form of a buffer tank was installed right after the syringe pump. The cut view and thermocouple location in the micro-channel test section is illustrated in Fig. 3. To reduce heat loss, G-7 fiber glass reinforced silicone was used to house the testing piece, and Marinat-P ceramic fiber board, which is machine-able, were applied for insulation. In addition, fiber glass wool was wrapped around for further insulation. As a result, heat loss of the system is within 5% of the energy balance calculation. Aluminum 2024 (24 mm by 24 mm) was used for the heating block as well as the micro-channel blocks. Type K sheathed thermocouples (508 μm diameter) and pressure transducers were placed at the inlet and outlet plenums to measure inlet and outlet pressure and pressure drop. Four more of type K sheathed thermocouples were buried at 890 μm below the test surface and positioned at the distances of 8, 12, 16, and 20 mm from the inlet of micro-channel. The data acquisition system is the National Instrument SCXI-1000 with SCXI-1102 module connected by TBX-1303 32 channels terminal block. The uncertainties of flow rate and pressure are ± 2% of the full scale for the rotameter and ± 0.25% of the full scale for the pressure transducer, respectively. The uncertainty of temperature is ± 2°C. The error of HP 34401A multimeter is

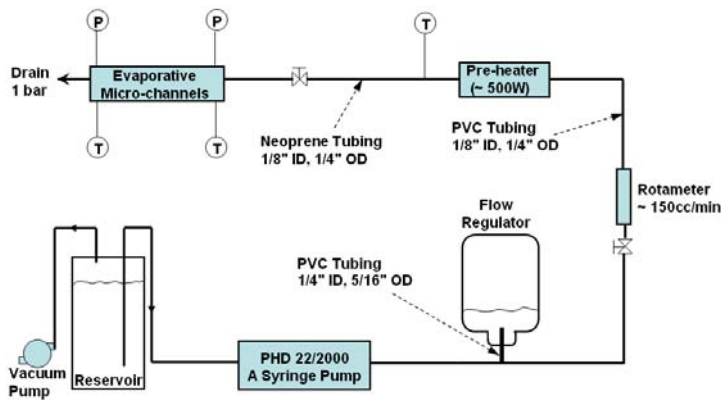


FIGURE 2. SYSTEM DIAGRAM OF EXPERIMENTAL SETUP

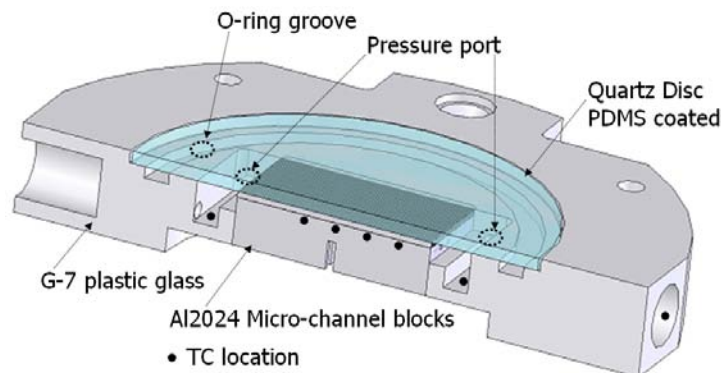
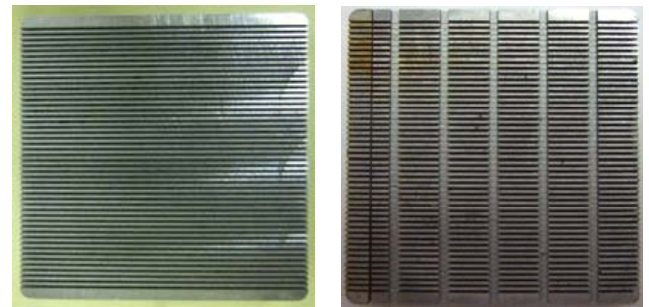


FIGURE 3. CUT VIEW AND THERMOCOUPLE LOCATION OF TEST SECTION

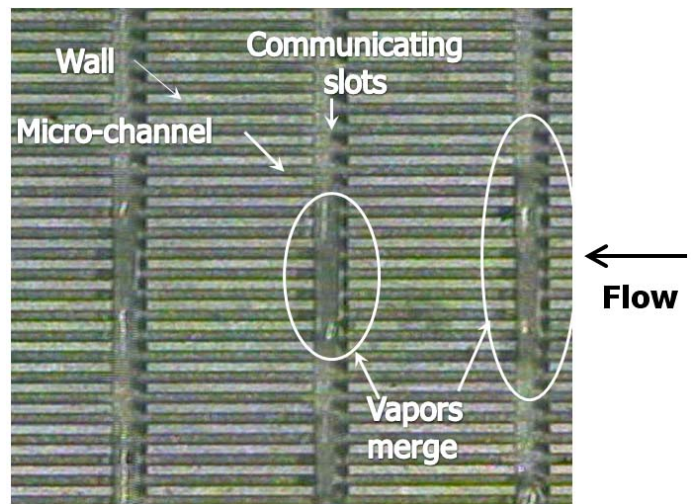
0.0015% and 0.06% for DC and AC, respectively. Total heat mount was measured by the multimeter, so that the error of heat heat flux was regarded as 0.06%. After considering maximum 5 % heat loss in the system, the uncertainty of heat loss is ± 0.6 % by the RSS method.

Among the various design of test sections, parallel and cross-cutting micro-channels block were selected in this study to demonstrate the non-uniform flows on the heat sink. The parallel micro-channel block has 48 parallel channels, with 235 μm channel width and 710 μm channel height, as shown in Fig. 4(a). The effectiveness of the flow instability parameter, R , of parallel micro-channels was validated by Lee et al. [1]. On the other hand, the cross-cutting micro-channels having five grooves which allow parallel channels to communicate is shown in Fig. 4(b). It is noticed that the width of the groove was made to be wider than the width of the micro-channels. Therefore, the vapor bubbles in the micro-channels will tend to migrate into the cross-cutting grooves due to the surface tension differential.

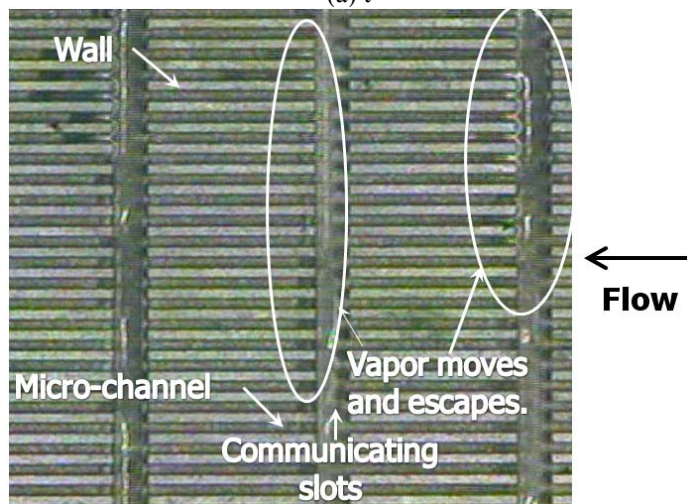
Figure 5 shows two-phase flow visualization in parallel micro-channels with cross-cutting grooves for the condition of heat flux 7 W/cm², inlet subcooling 10 °C, and mass flux 41.8 kg/m²/s [1]. Even if a bubble may expand violently in a segment of parallel micro-channels, they merged together in a cross-cutting groove, and are not able to continue immediately



(a) Parallel (b) Cross-cutting
FIGURE 4. TESTED MICRO-CHANNEL BLOCKS



(a) t



(b) t+0.5sec

FIGURE 5. TWO-PHASE FLOW VISUALIZATION IN CROSS-CUTTING MICRO-CHANNELS (41.8 KG/M²/S, 7 W/CM², AND 10 °C INLET SUBCOOLING)

into the up or downstream segments. After the bubbles merge in the cross-cutting grooves, they ran into the downstream segment of the micro-channels uniformly. Through experiments of the micro-channels with the cross-cutting grooves, flow

instability does not appear. Also, very little channel-to-channel difference was observed in the tests. Therefore, cross-cutting grooves are found experimentally to be effective at avoiding channel instability and channel-to-channel difference. Based on this experimental evidence, cross-cutting micro-channels are also expected to minimize the uneven flow distribution in parallel evaporative micro-channels when it is at non-uniform heating.

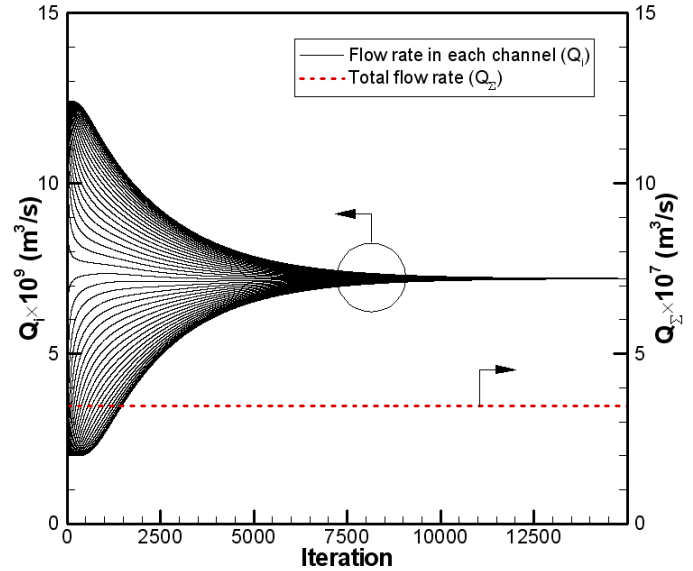
NETWORK SIMULATIONS

Three cases are modeled using evaporative micro-channel network analysis: as shown in Fig. 4, forty eight parallel micro-channels with uniform heating, with non-uniform heating, and cross-cutting micro-channels with non-uniform heating. The uniform heat flux and mass flux were 7 W/cm^2 and $41.8 \text{ kg/m}^2\text{/s}$, respectively. Inlet quality and pressure was given as zero ($x=0$) to make the network calculation simple. The system pressure is at 1.1 bar. For the case of non-uniform heating, a local hot spot which has additional 7 W/cm^2 applied at the zone, which starts at $1/3$ of channel length from the inlet and ending at $2/3$ of channel length in the micro-channel # 17 – 32.

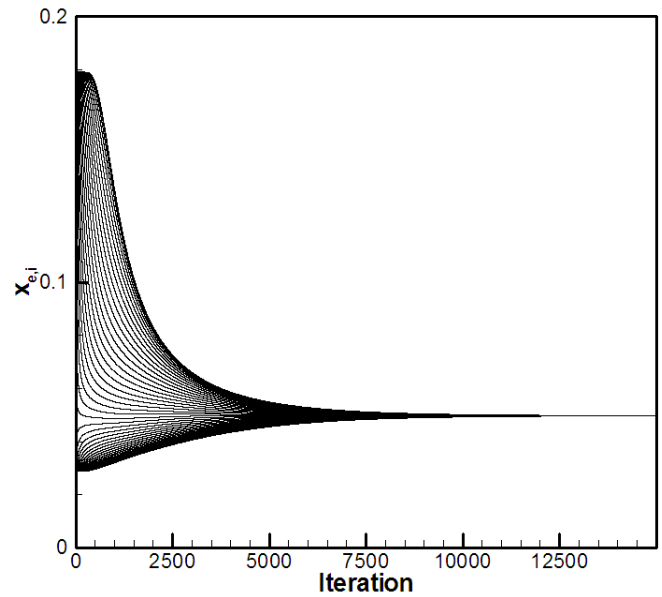
Parallel Micro-channels

To validate the evaporative micro-channel network model, two examples of network calculation were conducted. The first is of forty seven loops on the forty eight parallel micro-channels with 7 W/cm^2 uniform heating, as shown in Fig. 4(a). The total inlet volume flow rate was $3.46 \times 10^{-7} \text{ m}^3\text{/s}$ (or at $41.8 \text{ kg/m}^2\text{/s}$ mass flux). In the network analysis, the initial condition of inlet flow rate in each channel was randomly selected. However, a same flow rates is expected after evaporative micro-channel network calculation is completed due to the same two-phase head-losses for all the micro-channel 1 to 48. The exit quality, the ratio of vapor mass to total mass at the exit of parallel micro-channel, should also be same. As shown in Fig. 6(a) and (b), after 13,000 iterations of the Eqs. (9) and (10) the flow rates and exit qualities among all the micro-channels converged into the same flow rate and quality of $7.2 \times 10^{-9} \text{ m}^3\text{/s}$ and 0.05, respectively.

The second example is same parallel micro-channel system as the first example. However, except the uniform heat flux, an additional non-uniform heat flux is applied to the center $1/3$ length in the micro-channel # 17 – 32. Due to the non-uniform extra heating in the central channels, the two-phase head-loss in these channels is increased. The total inlet volume flow rate in this case was selected to be same as the previous example of uniform heating. The initial condition of inlet flow rate was also set randomly as before. Figure 7(a) shows the history of the flow rate convergence. After 4,000 iterations, the flow rate converged in each micro-channel. Because there were a local hot spot with 14 W/cm^2 heat flux on the center $1/3$ length in the non-uniformly heated zone, the local quality is increased and the two-phase pressure multiplier of the channels # 17 – 32 is greater than those of uniformly heated zone. Therefore, the



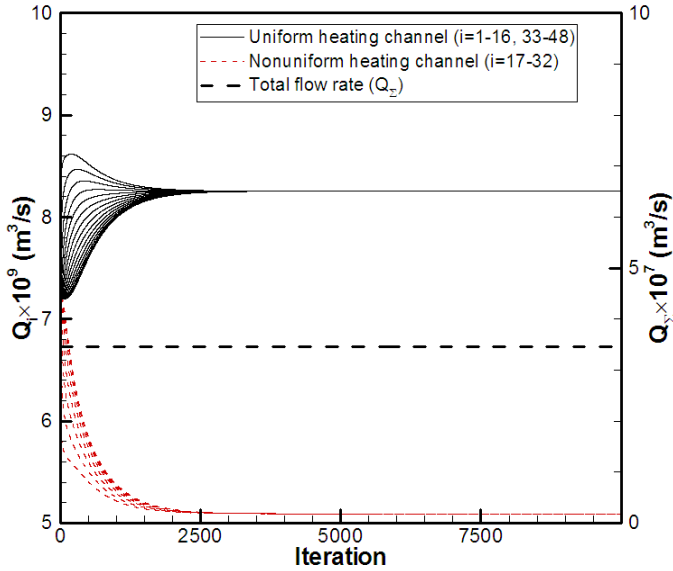
(a) Flow rate in each channel and total flow rate



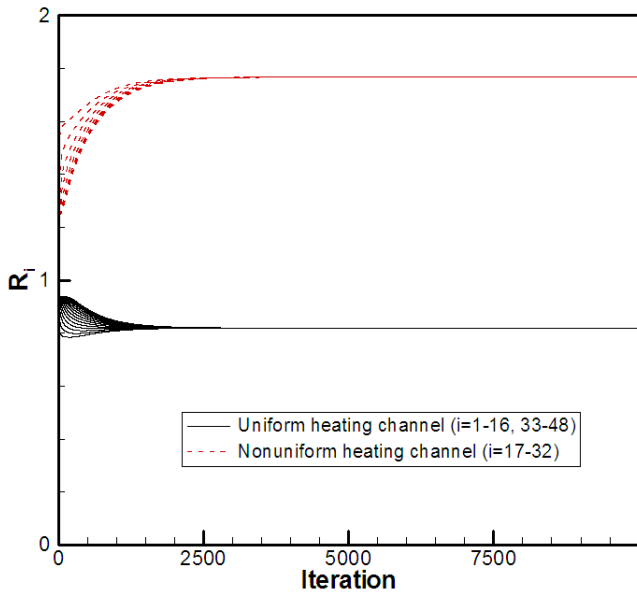
(b) Exit quality in each channel

FIGURE 6. CONVERGING RESULTS OF 47 LOOPS OF PARALLEL EVAPORATIVE MICRO-CHANNELS WITH UNIFORM HEATING

flow rate is smaller at $5.1 \times 10^{-9} \text{ m}^3\text{/s}$. For the uniformly heated zone of micro-channels, the flow rate was higher at $8.26 \times 10^{-9} \text{ m}^3\text{/s}$ caused by the lower quality and smaller friction multiplier. The corresponding exit quality is 0.043 and 0.094 for non-uniform heated and the uniform heated channels, respectively. Figure 7 (b) shows convergence of the instability parameter. If the instability parameter is less than 1, the evaporative micro-channel system would be stable. Based on the evaluation of the instability parameter, the maximum R value of this system is 1.77 and occurs in the non-uniform heated zone. Therefore, this overall evaporative micro-channel with non-uniform heating is not stable.



(a) Flow rate in each channel and total flow rate



(b) Instability parameter in each channel

FIGURE 7. CONVERGING RESULTS OF 47 LOOPS OF PARALLEL EVAPORATIVE MICRO-CHANNELS WITH NON-UNIFORM HEATING

Cross-cutting micro-channels

Evaporative network calculation was also applied to the case of cross-cutting micro-channels at non-uniform heating. To compare with parallel micro-channels, the modeling condition was selected to be the same as the second example of previous section. Figures 8 and 9 show the heat transfer coefficient and wall temperature along the micro-channel length in both parallel and cross-cutting micro-channels at non-uniform heating. It is noticed that both the heat transfer coefficient and the wall temperature have discontinuity at the

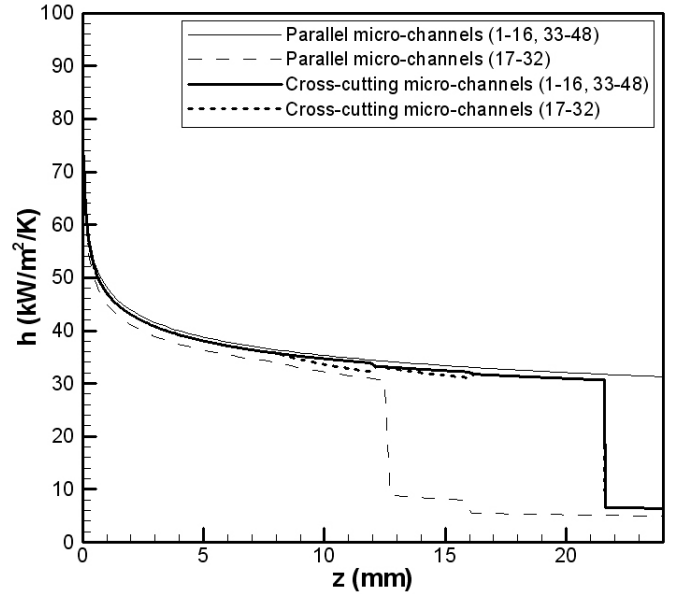


FIGURE 8. HEAT TRANSFER COEFFICIENT COMPARISON ALONG CHANNEL LENGTH IN PARALLEL AND CROSS-CUTTING MICRO-CHANNELS WITH NON-UNIFORM HEATING

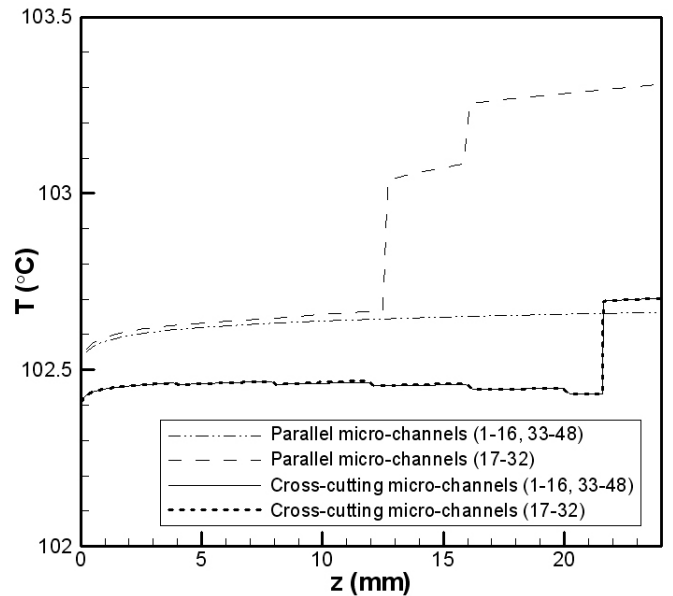


FIGURE 9. WALL TEMPERATURE COMPARISON ALONG LENGTH IN PARALLEL AND CROSS-CUTTING MICRO-CHANNELS WITH NON-UNIFORM HEATING

quality of 0.05. This is because the Lee et al.'s generalized heat transfer correlation [5] is based upon the Lee and Mudawar's heat transfer correlation [6].

Lee and Mudawar [6] separated the flow boiling mechanisms into three stages, divided by qualities at 0.05 and 0.55. At a lower quality ($x < 0.05$), the heat transfer coefficient is determined by the Martinelli parameter, X , because nucleate boiling dominates. In the medium quality stage ($0.05 < x < 0.55$),

the heat transfer coefficient not only depends on the Martinelli parameter, but also the Boiling and Weber numbers. Meanwhile, in the high quality stage ($x > 0.55$), the heat transfer coefficient is decided by a traditional film boiling correlation.

Figure 8 shows the two-phase heat transfer coefficient decreases, because the quality increases, along the channel length. The heat input in the non-uniform heated micro-channels # 17 – 32 is larger than that in the uniformly heated zone (channels # 1 – 16 and # 33 – 48) that their quality is higher and flow rate is lower. As a result in the case of parallel channels the heat transfer coefficient is reduced when quality exceeds 0.05. However, the cross-cutting micro-channels show almost the same heat transfer coefficient along each micro-channel although the heating is non-uniform. Once the two-phase flows merge in the cross-cutting grooves, they mix together, average the quality and then redistribute into the down-stream segment. Therefore, cross-cutting micro-channels minimize the uneven flow and heat transfer variation in evaporative micro-channels with non-uniform heating.

Figure 9 shows the bottom wall temperature of micro-channels along the channel length in parallel and cross-cutting micro-channels at non-uniform heating. After smaller flow rate comes in parallel micro-channel # 17 – 32, the bottom wall temperature of micro-channels, T_{ch} rises up 0.7 °C. For cross-cutting micro-channels, however, the difference of the bottom wall temperatures between center channels and side channels is negligible. The rise of wall temperature at the fin base, T_b was in the range of 2 °C. Generally, the center region of parallel channels shows an obvious increase of wall temperature starts from $z = 12$ mm, while the wall temperature distribution is fairly uniform in the cross-cutting micro-channels.

CONCLUSION

A network analysis model of evaporative micro-channel systems with possible non-uniform heating and channel branching has been established. The model is used to validate the advantage of cross-cutting micro-channels, which was observed experimentally. Both wall temperature and heat transfer coefficient were calculated on three different cases (forty eight parallel micro-channels with uniform heating, with non-uniform heating, and with cross-cutting and non-uniform heating). The main conclusions are:

(1) The network analysis model of evaporative micro-channel systems was established, which included generalized two-phase heat transfer and pressure drop correlations of micro-channels [5] and static flow instability predictive capability.

(2) Based on experimental evidence, cross-cutting micro-channels minimize the uneven flow, wall temperature variation and flow instability in parallel evaporative micro-channels [1]. This phenomenon was also demonstrated in the network modeling.

(3) The network analysis model will be able to support conceptual and detailed designs of evaporative micro-channel systems for general applications.

ACKNOWLEDGEMENTS

This work was supported in part by the Pennsylvania Infrastructure Technology Alliance (PITA), a partnership of Carnegie Mellon, Lehigh University, and the Commonwealth of Pennsylvania's Department of Community and Economic Development (DCED).

REFERENCES

- [1] Lee, H. J., Liu, D. Y., Yao, S. C., 2010, "Flow Instability of Evaporative Micro-channels," *Int. J. Heat Mass Transfer*, 53 (9-10), pp. 1740-1749.
- [2] Watters, G. Z., 1984, *Analysis and Control of Unsteady Flow in Pipelines*, 2nd ed., Boston: Butterworths, Chap. 2.
- [3] Lee, H. J., Yao, S. C., 2008, "Stability Analysis and Network Design of Evaporative Micro-channels," *ASME Heat Transfer, Fluids, Energy, Solar & Nano Conf.*, Jacksonville, FL, HT2008-56337.
- [4] Cho, E. S., Choi, J. B., Yoon, J. S., Kim, M. S., 2010, "Experimental Study on Microchannel Heat Sinks Considering Mass Flow Distribution with Non-uniform Heat Flux Conditions," *Int. J. Heat Mass Transfer*, 53 (9-10), pp. 2159-2168.
- [5] Lee, H. J., Liu, D. Y., Alyousef, Y., Yao, S. C., 2010, "Generalized Two-phase Pressure Drop and Heat Transfer Correlations in Evaporative Micro/mini-channels," *Journal of Heat Transfer*, *Trans ASME*, 132 (4), pp. 041004-1-9.
- [6] Lee, J., Mudawar, I., 2005, "Two-phase Flow in High-Heat-Flux Micro-channel Heat Sink for Refrigeration Cooling Applications: Part II - Heat Transfer Characteristics," *Int. J. Heat Mass Transfer*, 48 (5), pp. 941-955.
- [7] Incropera, F. P., DeWitt, D. P., 1996, *Fundamentals of Heat and Mass Transfer*, 3rd ed., John Wiley & Sons, Chap. 3.